Article

Not peer-reviewed version

A Common Polymorphism in RNASE6 Impacts Its Antimicrobial Activity Toward Uropathogenic *Escherichia coli*

Raul Anguita , Guillem Prats-Ejarque , Mohammed Moussaoui , Brian Becknell , Ester Boix *

Posted Date: 9 November 2023

doi: 10.20944/preprints202311.0606.v1

Keywords: RNase; RNase 6; RNase k6; single nucleotide polymorphisms; antimicrobial peptides; urinary tract infections; uropathogenic Escherichia coli

Article

A Common Polymorphism in *RNASE6* Impacts Its Antimicrobial Activity toward Uropathogenic *Escherichia coli*

Raul Anguita [1,†], Guillem Prats-Ejarque [1,†], Mohammed Moussaoui [1], Brian Becknell [2,*] and Ester Boix [1,*]

[1] Department of Biochemistry and Molecular Biology, Faculty of Biosciences, Universitat Autònoma de Barcelona, Cerdanyola del Vallès, Spain
[2] Kidney and Urinary Tract Center, The Abigail Wexner Research Institute at Nationwide Children's, Columbus, OH USA
* Correspondence: Ester Boix, Department of Biochemistry and Molecular Biology, Faculty of Biosciences, Universitat Autònoma de Barcelona, Cerdanyola del Vallès, 08193 Bellaterra, Spain Email: Ester.Boix@uab.cat; Brian Becknell, Kidney and Urinary Tract Center, Abigail Wexner Research Institute at Nationwide Children's Hospital, 700 Children's Drive, Columbus, Ohio 43205 USA, Email: brian.becknell2@nationwidechildrens.org
† These authors contributed equally to this work.

Abstract: Human Ribonuclease (RNase) 6 is a monocyte and macrophage-derived protein with potent antimicrobial activity toward uropathogenic bacteria. The *RNASE6* gene is heterogeneous in humans due to the presence of single nucleotide polymorphisms (SNPs). *RNASE6* rs1045922 is the most common non-synonymous SNP, resulting in a G to A substitution that determines an arginine (R) to glutamine (Q) transversion at position 66 in the protein sequence. By structural analysis we observed that R66Q substitution significantly reduces the positive electrostatic charge at the protein surface. Here, we generated both recombinant RNase 6 -R66 and -Q66 protein variants and determined their antimicrobial activity toward uropathogenic *Escherichia coli* (UPEC), the most common cause of UTI. We found that the R66 variant, encoded by the major SNP rs1045922 allele, exhibited superior bactericidal activity in comparison to the Q66 variant. The higher bactericidal activity of R66 variant correlated with an increase in the protein lipopolysaccharide binding and bacterial agglutination abilities, while retaining the same enzymatic efficiency. These findings encourage further work to evaluate *RNASE6* SNP distribution and its impact in UTI susceptibility.

Keywords: RNase; RNase 6; RNase k6; Single nucleotide polymorphisms; antimicrobial peptides; urinary tract infections; uropathogenic *Escherichia coli*

1. Introduction

Bacterial urinary tract infections (UTI) afflict 150 million people annually worldwide[1], with a lifetime incidence of 50-60% in women[2], 25-30% of whom suffer recurrent UTI within six months[3]. Uropathogenic *Escherichia coli* (UPEC) is the most common cause of UTI, accounting for 80-90% of cases[1,3]. The risk of ascending UTI and pyelonephritis is elevated in young children, people with diabetes, and the geriatric population, and this can lead to acute kidney injury and chronic kidney disease due to renal scarring[4–6]. The choice of antibiotics to manage UTI has been limited by mounting antimicrobial resistance [7,8]. These circumstances drive the demand for novel measures to identify patients most at risk for UTI recurrence.

A greater understanding of the human immune response to UTI should yield insights into mechanisms that account for heightened susceptibility to infection along with new strategies to combat UTI. Experiments in preclinical models of UTI attest that the innate immune system is chiefly responsible for UPEC detection and clearance [9–11]. The innate immune system of the urinary tract

 doi:10.20944/preprints202311.0606.v1

relies upon a combination of pattern recognition receptors, complement activation, phagocyte recruitment, and antimicrobial peptides and proteins (AMPs) to detect and destroy invading uropathogens [10,12,13]. The antimicrobial mechanisms of AMPs include among others: membrane disruption, microbial agglutination, blockade of cell division, impaired ribosomal translation, and micronutrient sequestration [14–17]. *In vitro* and *in vivo* studies have implicated AMPs in host defense against UTI. AMPs are synthesized by multiple cell types in the urinary tract, including urothelial cells, renal intercalated cells, neutrophils, monocytes, and macrophages[12,18,19].

Mounting evidence suggests that AMP levels and antimicrobial properties are reduced in patients with recurrent UTI (rUTI). Urine from girls with rUTI contains lower levels of AMPs, such as RNase 4, RNase 7, and Lipocalin-2/NGAL, compared to healthy controls[20–22]. Such quantitative defects may have an underlying genetic basis, as patients with fewer copies of immune related genes such as the defensin *DEFA1A3* and *DMBT1* genes experience rUTI more frequently [23,24]. Moreover, non-synonymous single nucleotide polymorphisms (SNP) in AMP encoding genes can result in defective antimicrobial activity. Along these lines, a common SNP in *RNASE7* that encodes a Pro103 to Ala substitution (rs1263872) reduces its bactericidal activity toward UPEC and is more prevalent in children with UTI[25]. Altogether, these studies indicate promising roles for AMP levels and genotypes as new prognostic tools to identify patients at high risk for recurrence.

We previously identified RNase 6 as a monocyte and macrophage -derived AMP that is expressed in the urinary tracts of humans and mice [16]. RNase 6, also named RNase k6, was originally identified as an orthologue of bovine kidney RNase 2 when tracing the evolutionary divergence within the RNaseA superfamily[26], a family that groups proteins endowed with a diversity of host defense properties[27]. By structure-functional studies we demonstrated that RNase 6 antimicrobial mechanism mostly relies on its action at the bacteria envelope and is dependent on both surface exposed hydrophobic and cationic residues[28]. The protein is more active on Gram-negative bacteria, showing a high affinity for lipopolysaccharide (LPS)[28]. Interestingly, recombinant human and mouse RNase 6 proteins exhibited bactericidal activity toward uropathogenic *Escherichia coli* (UPEC) at low-micromolar concentrations [16]. Accordingly, *RNASE 6* transgenic mice are less susceptible to UPEC induced experimental UTI than non-transgenic controls[29]. In this study, we have characterized the most common non-synonymous *RNASE6* SNP in the human population and assessed its impact on RNase 6 antimicrobial activity toward UPEC.

2. Results

2.1. RNASE6 rs1045922 Is a Common, Non-Synonymous SNP That Alters RNase 6 Antimicrobial Activity

Since previous studies have identified associations between genetic variants in antimicrobial proteins and UTI, we hypothesized that a common coding SNP in *RNASE6* may impact its antimicrobial activity toward UPEC. We performed a query at the dbSNP (https://www.ncbi.nlm.nih.gov/snp/) and identified rs1045922 as the most common, nonsynonymous variant in the protein coding region of *RNASE6*, with a minor allele frequency of 0.25-0.3 in the global population. An overall analysis of the G>A frequency highlights significant differences among the main geographical subareas, with a more than 75% predominance of G over A in the African population and a more balanced distribution in the East and South Asian groups (Figure 1).

Preprints (www.preprints.org) | NOT PEER-REVIEWED | Posted: 9 November 2023 doi:10.20944/preprints202311.0606.v1

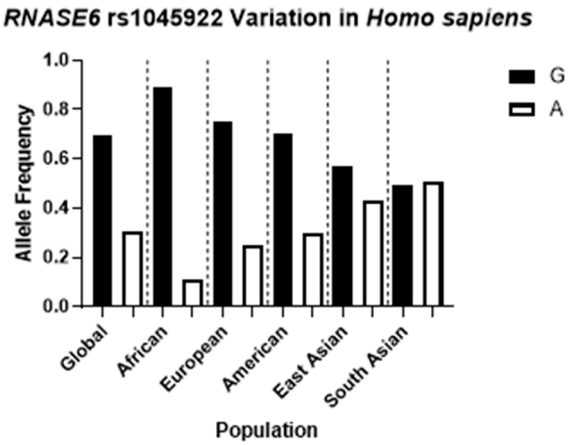

Figure 1. *RNASE6* rs1045922 SNP distribution among populations according to the 1000Genomes Study[30].

The minor allele confers a G-to-A nucleotide substitution, leading to an arginine to glutamine transversion at amino acid position 66 in the mature RNase 6 protein (i.e., R66Q). To test the influence of R66Q on the antimicrobial capacity of RNase 6, we generated and purified recombinant RNase 6-R66 and RNase 6-Q66 proteins. We found that RNase 6-R66 variant exhibited increased antimicrobial activity toward laboratory and clinical cystitis and pyelonephritis strains of *E. coli* (UTI89 and CFT073)[31,32], when compared to RNase 6-Q66 (Figure 2).

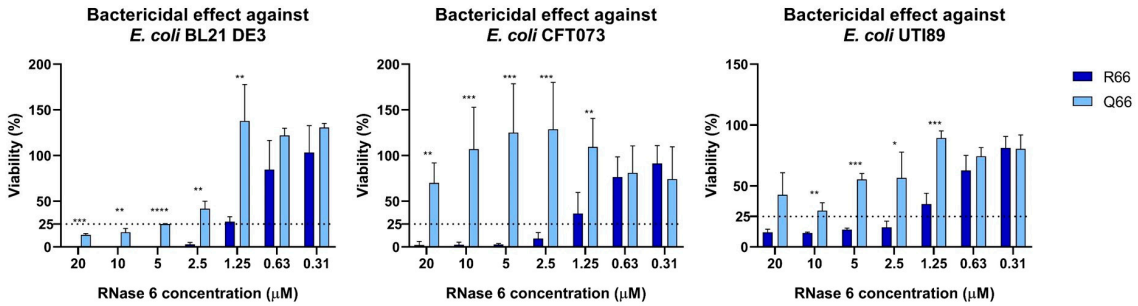

	E. coli BL21		*E. coli* CFT073		*E. coli* UTI89	
	MBC_{100}	MBC_{75}	MBC_{100}	MBC_{75}	MBC_{100}	MBC_{75}
RNase 6-R66	8.33 (±2.9)	2.08 (±0.72)	>20	1.87 (±0.68)	>20	3.33 (±1.44)
RNase 6-Q66	>20	8.22 (±2.9)	>20	>20	>20	>20

Figure 2. RNase 6-Q66 exhibits reduced antimicrobial activity toward laboratory and uropathogenic strains of *E. coli*, when compared with RNase 6-R66. Bacterial viability was performed by CFU counting taking the non-treated control as a 100% reference. Significant difference between the variants at each concentration is indicated (**** p<0.0001; *** p<0.0002; ** p<0.002; * p<0.03). The table below indicates the calculate Minimum Bactericidal Concentration (MBC) at which 100 or 75% of bacteria was eradicated. Each assay was performed at least in triplicate. Values denote mean ± standard error of the mean (SEM).

Mechanistically, RNase 6-Q66 displayed reduced LPS binding affinity and *E. coli* agglutination (Table 1) compared to the RNase6-R66 protein. Both of these properties are essential mechanisms implicated in the antimicrobial action of RNase 6 [28].

Preprints (www.preprints.org) | NOT PEER-REVIEWED | Posted: 9 November 2023 doi:10.20944/preprints202311.0606.v1

Table 1. LPS binding and Minimal Agglutination Concentration (MAC) for RNase 6 variants toward *E. coli*. LPS binding was assessed using the cadaverine-BODIPY TR (BC) fluorescent probe. EC_{50} indicates the protein concentration that achieves 50% effective BC displacement and "Max" refers to the maximum binding percentage (%), where 100% corresponds to total displacement and 0 corresponds to no displacement of the fluorescent dye. Three independent measurements were performed for each condition. Values denote mean ± SEM.

	LPS binding		MAC
	EC_{50} (µM)	Max (%)	(µM)
RNase 6-R66	2.64 ± 0.23	75.90 ± 4.41	0.22 ± 0.05
RNase 6-Q66	5.15 ± 2.8	29.71 ± 10.5	1.38 ± 0.24

2.2. Both SNP RNase6-R66 and -Q66 Display the Same Catalytic Activity

In contrast, the Arg to Gln substitution at position 66 did not have any effect on the protein catalytic activity, as evaluated by comparison of the initial velocities toward dinucleotide substrates (Table 2). Equivalent activities were registered for both UpA and CpA, whereas no detectable activity was observed for UpG, as previously reported for RNase6-R66 [33]. Both variants retained an equivalent U/C specificity at the main substrate base site (B1) and selectivity for adenine at the secondary site (B2).

Table 2. Comparison of the relative catalytic activity of the two RNase 6 variants.

	UpA	UpG	CpA
RNase 6-R66	100	N.D	100
RNase 6-Q66	87.5	N.D	92

ND Not Detected at the assayed conditions. Data expressed in% activity relative to RNase 6-R66 based on mean V_0 values of triplicate assays.

2.3. The RNase6 R66Q Substitution Significantly Reduces the Positive Electrostatic Charge at the Protein Surface

Finally, we predicted the influence of R66Q substitution within the RNase 6 3D environment. Based on the RNase 6 crystal structure solved at atomic resolution [33], R66 is a residue located at the protein surface, where it participates along with the neighboring H67 residue in a cationic cluster that interacts with both sulphate and phosphate anions (Figure 3A)[33,34]. The 3D structure of the RNase6-Q66 variant was predicted using the *AlphaFold2* server[35]. Simulation of the impact of its substitution with a non-charged amino acid (Q66) clearly illustrated how the arginine to glutamine substitution significantly reduced the positive electrostatic charge of the surface exposed region (Figure 3B). A close inspection of the structure indicates that R66Q not only leads to the loss of net cationic charge but also prevents the residue interaction with the anionic D107 residue (Figure S1A). Therefore, a significant reduction of the local surface cationic patch in the Q66 variant could diminish the protein's affinity for the anionic components within the bacterial wall.

Preprints (www.preprints.org) | NOT PEER-REVIEWED | Posted: 9 November 2023 doi:10.20944/preprints202311.0606.v1

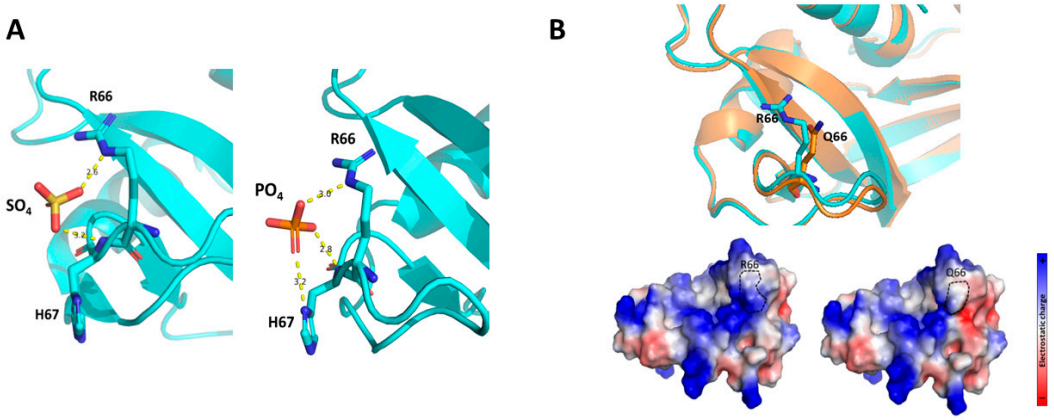

Figure 3. Analysis on the impact of the R66Q substitution on the protein structure. (**A**) Details of sulphate and phosphate binding interactions of RNase 6-R66 in solved crystal structures (PDB ID: 4X09 and 5OAB respectively). (**B**) The substitution of an arginine by a non-charged amino acid at the protein surface alters the cationic charge of this region, which in turn may disturb the ability of RNase 6 to bind to anionic bacterial wall components. The mutant structural prediction was obtained by *AlphaFold2*. Top: RNase 6-R66 is shown in cyan while the -Q66 variant is shown in orange. Bottom: Surface electrostatic charge prediction. The position corresponding to the amino acid change is indicated by the dotted black line. Pictures were drawn with *PyMol* 2.3.4.

Thus, structural analysis supports the present experimental data showing that the SNP that encodes for R66Q substitution determines a significant reduction in its LPS binding, bacteria agglutination and overall antimicrobial activities.

3. Discussion

While the human genome exhibits considerable diversity particularly in its compendium of genes associated with innate immunity, the functional implications of this diversity in many cases have not been fully addressed[14,36]. Mounting evidence indicates that differences in UTI susceptibility among humans may have a genetic basis[23–25]. Within the RNase A superfamily, some SNPs have been associated with disease predisposition and infection susceptibility[25,37–39].In this study, we focused on the functional consequences of the most common, non-synonymous SNP in *RNASE6* on its antimicrobial properties toward UPEC, the most common cause of bacterial UTI.

The comparison of the antimicrobial properties of the resulting RNase 6-Q66 and RNase6-R66 variants toward UPEC strains illustrated significant differences (Figure 2). RNase 6 antimicrobial potency has been partly associated with its capacity to bind to LPS at the bacterial cell wall and agglutinate cells[28]. In this regard, it is noteworthy that RNase 6-Q66, the minor variant (Figure 1), was less effective in LPS binding and *E. coli* agglutination when compared to the predominant RNase 6-R66 protein (Table 1). A close structural inspection revealed that R66 contributes to a cationic region that favors anion ligand binding (Figure 3), as observed in the solved crystal structures of RNase 6 in complex with either sulphate or phosphate anions (PDB IDs: 4X09 and 5OAB)[33,34]. Indeed, the N64-R66 stretch was identified by PDBe motif as a cation region prone to bind anionic molecules, and R66 was identified as a key residue for the protein's putative saccharide binding by molecular modelling[40]. Likewise, the cationic residues at the protein surface were identified to interact with the anionic bacterial LPS in RNase 3, another RNase A family homologue with antimicrobial properties[41]. RNase binding to LPS was correlated to the induction of bacterial agglutination by screening a battery of LPS progressively truncated *E.coli* strains[42]. Thus, we posit that decreased surface cationic charge accounts for reduced LPS binding, *E. coli* agglutination, and microbicidal activity of RNase 6-Q66.

On the other hand, R66Q substitution did not alter the enzyme catalytic activity (Table 2). Kinetic results using dinucleotides as substrates did not reveal any significant in the catalytic efficiency or in

 doi:10.20944/preprints202311.0606.v1

the enzyme base preference. Although structural data indicates that the 64-68 loop is the main anchoring region for RNase 6 binding to adenine at the B2 site, residue 66 would not interact directly with the base ring. Recent solving of RNase 6 crystal structure in complex with an adenine mononucleotide revealed direct hydrogen bonding with N64 and N68, but no direct interaction with R66 [43]. Overlapping of the predicted 3D structure of the RNase6-Q66 variant onto the RNase6-R66 in complex with AMP (PDB ID: 6MV7) [43] suggests equivalent interactions with the nucleotide, where N64 and N68 in both variants could bind to the adenine ring and the neighbor R/Q66 residues cannot make direct interactions (Figure S1B). Previous structural analysis by molecular dynamics within the RNase A superfamily highlighted position 66 in RNase 6 as counterpart to Q69 in RNase A[33,44], where Q69 can complement the role of N71 (N68 in RNase 6). The prior work by molecular dynamics also highlighted the potential roles of both N64 and N68 for direct binding to adenine at B_2 but no direct contribution to R66[44]. Overlapping of RNase 6-AMP complex with RNase A- d(CpA) corroborates the equivalent roles of N64/N67 and N68/N71 in both RNases, but alternate orientation for R66 in RNase 6 and Q69 in RNase A (Figure S2). Besides, whereas R66 side chain in RNase 6 is determined by electrostatic interactions with D107 (Figure S1A), in the Q66 variant, the side chain might perform equivalent to Q69 in RNase A. Therefore, further work would be needed to fully evaluate the implications of R66Q substitution on RNase 6 substrate selectivity.

Interestingly, evolutionary studies of RNase 6 lineage indicated an unusual low substitution rate in comparison to other family lineage types [45]. Among the few non-synonymous substitutions we observe a trend for Gln to Arg substitution at position 66 from lower to higher order primates, which correlates with a slight increase in the protein cationicity [45]. In fact, position 66 stands out as RNase 6 lineage specific when mapping the sequence evolutionary rates among the RNase A superfamily homologues using the *Consurf* server (Figure S3A)[46]. Whereas R66 is conserved in the 4 hominid species, all the old-world monkeys have a Gln at this position (Figure S3B) and the new-world monkeys present significant differences at this region, with overall an average lower estimated pI [45]. Further work would be required to consider the functional significance of sequence diversity at this location.

Our query of dbSNP identified *RNASE6* rs1045922 as the most common, non-synonymous SNP in the human population. Studies are warranted to examine *RNASE6* rs1045922 genotypes in combination with other common variants in genes associated with the innate immune response in patients with UTI. Such studies will benefit from examination of additional, common SNP haplotypes within *RNASE6* and more broadly within the RNase A Superfamily, such as the *RNASE7* rs1263872 polymorphism recently associated with UTI susceptibility [25], as it is plausible that combinations of these SNP converge to impact UTI risk.

In this study, we have identified *RNASE6* rs1045922 as a common, functionally significant SNP within the human population and implicated R66 as a key amino acid residue for the antimicrobial potency of RNase 6 toward UPEC. Additional work is envisaged to consider the association of this and other *RNASE6* SNPs with UTI susceptibility.

4. Materials and Methods

Materials

Isopropyl _-D-1-thiogalactopyranoside (IPTG), was from Apollo Scientific (Bredbury, Chesire, UK). LPS from E. coli serotype 0111:B4 (type XII) were purchased from Sigma-Aldrich (St. Louis, MO, USA). BODIPY® cadaverine (BC) was from Molecular Probes (Eugene, OR, USA). CpA, UpA and UpG were from IBA Life Sciences. *Escherichia coli* BL21 was purchased at *Novagen*, Madison, WI, USA). UTI89 is a clinical UPEC isolate from a patient with cystitis[31]. CFT073 is a clinical UPEC isolate from a patient with pyelonephritis and urosepsis[32]. All strains were inoculated from glycerol stocks and grown statically in LB medium for 16 hours at 37°C.

 doi:10.20944/preprints202311.0606.v1

Expression of RNase6-R66 and -Q66 Variants

The RNase 6-Q66 variant was generated by site-directed mutagenesis[28]. Recombinant proteins were expressed and purified from inclusion bodies as previously described[28]. Briefly, the genes were subcloned into the plasmid pET11c for prokaryote high yield expression in an *E. coli* BL21(DE3) strain. Bacteria were grown in Terrific broth (TB), containing 400 µg/mL ampicillin. Recombinant protein was expressed after cell induction with 1 mM IPTG added when the culture showed an OD600 of 0.6. The cell pellet was collected after 4 h of culture at 37° C. Following bacteria cell lysis and solubilization of inclusion bodies, the protein was then refolded for 72 h at 4 °C by a rapid 100-fold dilution into 100 mM Tris/HCl, pH 8.5, 0.5 M of guanidinium chloride, and 0.5 M L-arginine, and oxidized glutathione (GSSG) was added to obtain a DTT/GSSG ratio of 4. The folded protein was then concentrated, buffer-exchanged against 150 mM sodium acetate, pH 5, and purified by cation-exchange chromatography on a Resource S (GE Healthcare) column equilibrated with the same buffer. The protein was eluted with a linear NaCl gradient from 0 to 2 M in 150 mM sodium acetate, pH 5.

Minimum Bactericidal Concentration (MBC) Determination

Minimal Bactericidal Concentration (MBC) was determined as previously[47]. Briefly, an exponential phase bacterial subculture adjusted to 5 x 10^5 CFU/mL in Hepes Buffer Saline (HBS) was incubated with recombinant RNase serially diluted from 20 to 0.31 µM during 4h at 37 ºC in mild agitation (100 rpm). Treatments were performed in a 96 well plate in 100 µL of volume. After incubation, 30 µL of the wells content is seeded into LB Petri dishes and incubated overnight at 37 ºC for colony counting.

Lipopolysaccharide Binding Assay

Lipopolysaccharide (LPS) binding was determined using the cadaverine-BODIPY TR (BC) fluorescence assay, where BC displacement was monitored. Serial protein dilutions were prepared in a 96-wells fluorescence plate from 20 µM, in HEPES 10 mM pH 7.4. Then, LPS (10 µg/mL) and BC (10 µM) were added in each well and the fluorescence was read on a Victor3 plate reader (PerkinElmer, Waltham, MA) with an excitation wavelength of 580 nm and 620 nm of emission. Fluorescence of free BC was registered and the binding to LPS was calculated as previously[48].

Bacterial Agglutination Assay

Bacterial agglutination was determined by calculation of the Minimal Agglutination Concentration (MAC) as previously[28]. Briefly, serial dilutions of the proteins were prepared on a 96-well ELISA plate in PBS, starting at 10 µM. Negative controls containing only buffer instead of protein, and bacteria were added to all wells with a final OD600 of 0.2 (5x10^5 CFU/mL). Then, the plates were incubated for 4 hours at 37º C and the bacterial aggregates were observed using a binocular stereo microscope at 50x. The MAC was defined as the lowest concentration where agglutinates could be seen. Three independent repeats of each assay were performed.

Spectrophotometric Kinetic Assay

Enzymatic activity was assayed by spectrophotometry as previously described[33]. Briefly, dinucleotides (IBA Life Sciences) were used as substrates and assays were carried out in 50 mM sodium acetate and 1mM EDTA, pH 5.5, at 25 °C, using 1-cm path length cells. The activity was measured by following the initial reaction velocities using the difference molar absorbance coefficients, in relation to the cleaved phosphodiester bonds. The relative activity was calculated by comparison of initial velocities (V_0) using a substrate concentration of 100 µM.

3D Structure Prediction

The R66Q model was predicted using the *AlphaFold2* server [35,49] based on the solved 3D structure of RNase 6-R66[33]. Five equivalent output models were generated with more than 90% liability over the whole protein sequence.

Supplementary Materials: The following supporting information can be downloaded at the website of this paper posted on Preprints.org. Figure S1A. Comparison of the local 3D structure of RNase 6-R66 and Q66 variants. Figure S1B. Comparison of the predicted 3D RNase 6-Q66 structure superimposed onto the RNase 6-R66-AMP complex (PDB ID:6MV7). Figure S2. Comparison of the 3D structure of RNase 6-R66 -AMP complex (PDB ID: 6MV7) superimposed onto the RNase A- d(CpA) complex (PDB ID:7RPG). Figure S3A: Analysis of conserved and variable residues in the RNase 6 primary sequence based on 300 RNase A family sequence homologues. Figure S3B. Sequence alignment of RNase 6 homologues within primates, showing the amino acid variability at the environament of amino acid position 66.

Author Contributions: For research articles with several authors, a short paragraph specifying their individual contributions must be provided. The following statements should be used "Conceptualization, E.B. and B.B.; methodology, E.B., R.A:, G.P-E., M.M.; data curation, R.A., E.B. and B.B.; writing—original draft preparation, B.B and E.B..; writing—review and editing, E.B. and B.B.; supervision, E.B., B.B., M.M. and G. P-E.; funding acquisition, E.B. and B.B. All authors have read and agreed to the published version of the manuscript."

Funding: This research was funded by the National Institutes of Health (NIDDK) R03 DK118306 (BB) and the *Agencia Estatal de Investigación*, Spain to EB (PID2019-106123GB-I00/AEI/10.13039/501100011033).

Institutional Review Board Statement: "Not applicable".

Data Availability Statement: Any data supporting the reported results can be provided upon request.

Acknowledgments: We acknowledge Helena Carbó (Dpt. Biochemistry and Molecular Biology, UAB) for technical support and Dr. Molly Ingersoll (Institut Pasteur, Paris, France) for providing the UTI89 strain.

Conflicts of Interest: The authors declare no conflict of interest.

References

1. Flores-Mireles AL, Walker JN, Caparon M, Hultgren SJ. 2015. Urinary tract infections: epidemiology, mechanisms of infection and treatment options. *Nat Rev Microbiol* 13: 269-84
2. Medina M, Castillo-Pino E. 2019. An introduction to the epidemiology and burden of urinary tract infections. *Ther Adv Urol* 11: 1756287219832172
3. Foxman B. 2014. Urinary tract infection syndromes: occurrence, recurrence, bacteriology, risk factors, and disease burden. *Infect Dis Clin North Am* 28: 1-13
4. Johnson JR, Russo TA. 2018. Acute Pyelonephritis in Adults. *N Engl J Med* 378: 48-59
5. Becknell B, Schober M, Korbel L, Spencer JD. 2015. The diagnosis, evaluation and treatment of acute and recurrent pediatric urinary tract infections. *Expert Rev Anti Infect Ther* 13: 81-90
6. Korbel L, Howell M, Spencer JD. 2017. The clinical diagnosis and management of urinary tract infections in children and adolescents. *Paediatr Int Child Health* 37: 273-9
7. Paul R. 2018. State of the Globe: Rising Antimicrobial Resistance of Pathogens in Urinary Tract Infection. *J Glob Infect Dis* 10: 117-8
8. Abbott IJ, Peel TN, Cairns KA, Stewardson AJ. 2023. Antibiotic management of urinary tract infections in the post-antibiotic era: a narrative review highlighting diagnostic and antimicrobial stewardship. *Clin Microbiol Infect* 29: 1254-66
9. Kuhn HW, Hreha TN, Hunstad DA. 2023. Immune defenses in the urinary tract. *Trends Immunol* 44: 701-11
10. Ching C, Schwartz L, Spencer JD, Becknell B. 2020. Innate immunity and urinary tract infection. *Pediatr Nephrol* 35: 1183-92
11. Lacerda Mariano L, Ingersoll MA. 2020. The immune response to infection in the bladder. *Nat Rev Urol* 17: 439-58
12. Becknell B, Schwaderer A, Hains DS, Spencer JD. 2015. Amplifying renal immunity: the role of antimicrobial peptides in pyelonephritis. *Nat Rev Nephrol* 11: 642-55

13. Ali AS, Townes CL, Hall J, Pickard RS. 2009. Maintaining a sterile urinary tract: the role of antimicrobial peptides. *J Urol* 182: 21-8
14. Lazzaro BP, Zasloff M, Rolff J. 2020. Antimicrobial peptides: Application informed by evolution. *Science* 368
15. Becknell B, Ching C, Spencer JD. 2019. The Responses of the Ribonuclease A Superfamily to Urinary Tract Infection. *Front Immunol* 10: 2786
16. Becknell B, Eichler TE, Beceiro S, Li B, Easterling RS, Carpenter AR, James CL, McHugh KM, Hains DS, Partida-Sanchez S, Spencer JD. 2015. Ribonucleases 6 and 7 have antimicrobial function in the human and murine urinary tract. *Kidney Int* 87: 151-61
17. Wang G, Mishra B, Lau K, Lushnikova T, Golla R, Wang X. 2015. Antimicrobial peptides in 2014. *Pharmaceuticals (Basel)* 8: 123-50
18. Chromek M, Slamova Z, Bergman P, Kovacs L, Podracka L, Ehren I, Hokfelt T, Gudmundsson GH, Gallo RL, Agerberth B, Brauner A. 2006. The antimicrobial peptide cathelicidin protects the urinary tract against invasive bacterial infection. *Nat Med* 12: 636-41
19. Spencer JD, Schwaderer AL, Wang H, Bartz J, Kline J, Eichler T, DeSouza KR, Sims-Lucas S, Baker P, Hains DS. 2013. Ribonuclease 7, an antimicrobial peptide upregulated during infection, contributes to microbial defense of the human urinary tract. *Kidney Int* 83: 615-25
20. Forster CS, Johnson K, Patel V, Wax R, Rodig N, Barasch J, Bachur R, Lee RS. 2017. Urinary NGAL deficiency in recurrent urinary tract infections. *Pediatr Nephrol* 32: 1077-80
21. Eichler T, Bender K, Murtha MJ, Schwartz L, Metheny J, Solden L, Jaggers RM, Bailey MT, Gupta S, Mosquera C, Ching C, La Perle K, Li B, Becknell B, Spencer JD. 2019. Ribonuclease 7 Shields the Kidney and Bladder from Invasive Uropathogenic Escherichia coli Infection. *J Am Soc Nephrol* 30: 1385-97
22. Bender K, Schwartz LL, Cohen A, Vasquez CM, Murtha MJ, Eichler T, Thomas JP, Jackson A, Spencer JD. 2021. Expression and function of human ribonuclease 4 in the kidney and urinary tract. *Am J Physiol Renal Physiol* 320: F972-F83
23. Hains DS, Polley S, Liang D, Saxena V, Arregui S, Ketz J, Barr-Beare E, Rawson A, Spencer JD, Cohen A, Hansen PL, Tuttolomondo M, Casella C, Ditzel HJ, Cohen D, Hollox EJ, Schwaderer AL. 2021. Deleted in malignant brain tumor 1 genetic variation confers urinary tract infection risk in children and mice. *Clin Transl Med* 11: e477
24. Schwaderer AL, Wang H, Kim S, Kline JM, Liang D, Brophy PD, McHugh KM, Tseng GC, Saxena V, Barr-Beare E, Pierce KR, Shaikh N, Manak JR, Cohen DM, Becknell B, Spencer JD, Baker PB, Yu CY, Hains DS. 2016. Polymorphisms in alpha-Defensin-Encoding DEFA1A3 Associate with Urinary Tract Infection Risk in Children with Vesicoureteral Reflux. *J Am Soc Nephrol* 27: 3175-86
25. Pierce KR, Eichler T, Mosquera Vasquez C, Schwaderer AL, Simoni A, Creacy S, Hains DS, Spencer JD. 2021. Ribonuclease 7 polymorphism rs1263872 reduces antimicrobial activity and associates with pediatric urinary tract infections. *J Clin Invest* 131
26. Rosenberg HF, Dyer KD. 1996. Molecular cloning and characterization of a novel human ribonuclease (RNase k6): increasing diversity in the enlarging ribonuclease gene family. *Nucleic Acids Res* 24: 3507-13
27. Lu L, Li J, Moussaoui M, Boix E. 2018. Immune Modulation by Human Secreted RNases at the Extracellular Space. *Front Immunol* 9: 1012
28. Pulido D, Arranz-Trullen J, Prats-Ejarque G, Velazquez D, Torrent M, Moussaoui M, Boix E. 2016. Insights into the Antimicrobial Mechanism of Action of Human RNase6: Structural Determinants for Bacterial Cell Agglutination and Membrane Permeation. *Int J Mol Sci* 17: 552
29. Ruiz-Rosado JD. 2023. Human Ribonuclease 6 has a Protective Role During Experimental Urinary Tract Infection.
30. Genomes Project C, Auton A, Brooks LD, Durbin RM, Garrison EP, Kang HM, Korbel JO, Marchini JL, McCarthy S, McVean GA, Abecasis GR. 2015. A global reference for human genetic variation. *Nature* 526: 68-74
31. Mulvey MA, Schilling JD, Hultgren SJ. 2001. Establishment of a persistent Escherichia coli reservoir during the acute phase of a bladder infection. *Infect Immun* 69: 4572-9
32. Mobley HL, Green DM, Trifillis AL, Johnson DE, Chippendale GR, Lockatell CV, Jones BD, Warren JW. 1990. Pyelonephritogenic Escherichia coli and killing of cultured human renal proximal tubular epithelial cells: role of hemolysin in some strains. *Infect Immun* 58: 1281-9

33. Prats-Ejarque G, Arranz-Trullen J, Blanco JA, Pulido D, Nogues MV, Moussaoui M, Boix E. 2016. The first crystal structure of human RNase 6 reveals a novel substrate-binding and cleavage site arrangement. *Biochem J* 473: 1523-36
34. Prats-Ejarque G, Blanco JA, Salazar VA, Nogues VM, Moussaoui M, Boix E. 2019. Characterization of an RNase with two catalytic centers. Human RNase6 catalytic and phosphate-binding site arrangement favors the endonuclease cleavage of polymeric substrates. *Biochim Biophys Acta Gen Subj* 1863: 105-17
35. Bryant P, Pozzati G, Elofsson A. 2022. Improved prediction of protein-protein interactions using AlphaFold2. *Nat Commun* 13: 1265
36. Rivas-Santiago B, Serrano CJ, Enciso-Moreno JA. 2009. Susceptibility to infectious diseases based on antimicrobial peptide production. *Infect Immun* 77: 4690-5
37. Eriksson J, Reimert CM, Kabatereine NB, Kazibwe F, Ireri E, Kadzo H, Eltahir HB, Mohamed AO, Vennervald BJ, Venge P. 2007. The 434(G>C) polymorphism within the coding sequence of Eosinophil Cationic Protein (ECP) correlates with the natural course of Schistosoma mansoni infection. *Int J Parasitol* 37: 1359-66
38. Jonsson UB, Bystrom J, Stalenheim G, Venge P. 2002. Polymorphism of the eosinophil cationic protein-gene is related to the expression of allergic symptoms. *Clin Exp Allergy* 32: 1092-5
39. McLaughlin RL, Phukan J, McCormack W, Lynch DS, Greenway M, Cronin S, Saunders J, Slowik A, Tomik B, Andersen PM, Bradley DG, Jakeman P, Hardiman O. 2010. Angiogenin levels and ANG genotypes: dysregulation in amyotrophic lateral sclerosis. *PLoS One* 5: e15402
40. Boix E, Salazar VA, Torrent M, Pulido D, Nogues MV, Moussaoui M. 2012. Structural determinants of the eosinophil cationic protein antimicrobial activity. *Biol Chem* 393: 801-15
41. Pulido D, Garcia-Mayoral MF, Moussaoui M, Velazquez D, Torrent M, Bruix M, Boix E. 2016. Structural basis for endotoxin neutralization by the eosinophil cationic protein. *FEBS J* 283: 4176-91
42. Pulido D, Moussaoui M, Andreu D, Nogues MV, Torrent M, Boix E. 2012. Antimicrobial action and cell agglutination by the eosinophil cationic protein are modulated by the cell wall lipopolysaccharide structure. *Antimicrob Agents Chemother* 56: 2378-85
43. Narayanan C, Bernard DN, Letourneau M, Gagnon J, Gagne D, Bafna K, Calmettes C, Couture JF, Agarwal PK, Doucet N. 2020. Insights into Structural and Dynamical Changes Experienced by Human RNase 6 upon Ligand Binding. *Biochemistry* 59: 755-65
44. Prats-Ejarque G, Lu L, Salazar VA, Moussaoui M, Boix E. 2019. Evolutionary Trends in RNA Base Selectivity Within the RNase A Superfamily. *Front Pharmacol* 10: 1170
45. Deming MS, Dyer KD, Bankier AT, Piper MB, Dear PH, Rosenberg HF. 1998. Ribonuclease k6: chromosomal mapping and divergent rates of evolution within the RNase A gene superfamily. *Genome Res* 8: 599-607
46. Ashkenazy H, Abadi S, Martz E, Chay O, Mayrose I, Pupko T, Ben-Tal N. 2016. ConSurf 2016: an improved methodology to estimate and visualize evolutionary conservation in macromolecules. *Nucleic Acids Res* 44: W344-50
47. Prats-Ejarque G, Lorente H, Villalba C, Anguita R, Lu L, Vazquez-Monteagudo S, Fernandez-Millan P, Boix E. 2021. Structure-Based Design of an RNase Chimera for Antimicrobial Therapy. *Int J Mol Sci* 23
48. Torrent M, Navarro S, Moussaoui M, Nogues MV, Boix E. 2008. Eosinophil cationic protein high-affinity binding to bacteria-wall lipopolysaccharides and peptidoglycans. *Biochemistry* 47: 3544-55
49. Jumper J, Evans R, Pritzel A, Green T, Figurnov M, Ronneberger O, Tunyasuvunakool K, Bates R, Zidek A, Potapenko A, Bridgland A, Meyer C, Kohl SAA, Ballard AJ, Cowie A, Romera-Paredes B, Nikolov S, Jain R, Adler J, Back T, Petersen S, Reiman D, Clancy E, Zielinski M, Steinegger M, Pacholska M, Berghammer T, Bodenstein S, Silver D, Vinyals O, Senior AW, Kavukcuoglu K, Kohli P, Hassabis D. 2021. Highly accurate protein structure prediction with AlphaFold. *Nature* 596: 583-9